(Received 20 October 2025, Accepted 11 November 2025, Scheduled 18 December 2025)

Innovative Design and Investigation on Resistive and Capacitive Network Based NGD Topology

Runtao Song[1], Sonia Moussa[2, 3], Nathan B. Gurgel[4], Nicolas Waldhoff[5], Ali H. D. Fakra[6, 7], Dmitry Kholodnyak[8], Mathieu Guerin[9], Glauco Fontgalland[10], Fayu Wan[1], and Blaise Ravelo[1, *]

[1] *Nanjing University of Information Science & Technology (NUIST), Nanjing 210044, Jiangsu, China*
[2] *University of Antsiranana, Antsiranana 201, Madagascar*
[3] *LES, LR11ES15, University of Tunis El Manar, ENIT, Tunis, Tunisia*
[4] *Applied Electromagnetic and Microwave Laboratory, Federal University of Campina Grande, Campina Grande 58429, Brazil*
[5] *UDSMM, Unite de Dynamique de Structure des Materiaux Moleculaires, Université de Littoral Côte d'Opale, Calais, France*
[6] *University of Lorraine, INRAE, Laboratory for Studies and Research on Wood Materials (LERMAB), F-54000 Nancy, France*
[7] *University of Antananarivo, ESPA, Research Laboratory of Material, Process and Civil Engineering (LRMPGC) Sis Ambohitsaina BP 1500, Antananarivo 101, Madagascar*
[8] *Department of Microwave Electronics, Saint Petersburg Electrotechnical University "LETI", Saint Petersburg, Russia*
[9] *Aix-Marseille University, CNRS, University of Toulon, IM2NP UMR7334, Marseille 13007, France*
[10] *Brenton School of Engineering, University of Mount Union, Alliance, OH 44601, USA*

ABSTRACT: This paper investigates the circuit theory of elementary passive topology exhibiting reconfigurable positive/negative delay (RPND) effect. This novel evaluated framework enables identification of the first-order L-topology constituted by RC-network operating under RPND effect. The investigated passive L-cell can operate in both negative and positive group delay (NGD or PGD) mode depending on the RC-network parameter. After establishing the NGD existence condition, the design equations versus the RPND effect including the target parameter values are formulated. To validate the theory, an RC-circuit representing a RPND Proof-of-Concept (PoC) was designed, implemented and tested especially in the time-domain by verifying the time-advance signature corresponding to the NGD operation mode. By tuning a PoC resistor, experimentation of pulse and arbitrary waveform signals confirm the feasibility to observe RPND reconfigurability. In the NGD mode, it is observed that outputs in time-advance of their own inputs about -3 ms. The RPND circuit is particularly useful for adjusting delay effect and signal synchronization in the communication system.

1. INTRODUCTION

The negative group delay (NGD) abnormal phenomenon was theoretically identified in the 1960s and was experimentally studied in the early 1980s by physicists [1, 2]. The initial study on the NGD abnormal effect was performed in optics wavelengths by using negative group velocity pulse propagation. Hence, the NGD effect was studied on superluminal optical systems [3, 4] with the latter interest of electronics and microwave research engineers in the 90s.

The experimentations of microwave circuits designed with diverse electronic topologies have shown the NGD existence at gigahertz (GHz) frequencies [5–14]. However, the question whether the NGD circuit blocks are feasible or not in practical systems is raised. So far, the NGD electronic function is expected, among relevant solutions, to reduce the unintentional effect of group delay (GD) especially in the communication devices and components [15]. Meanwhile, the usefulness of NGD circuit application in communication engineering depends on the improvement of compactness [7], low-attenuation [8] and input matching. Therefore, NGD circuits based on distributed transmission line (TL) topologies were proposed for RF and microwave applications [9–14]. Ones of the most explored microwave NGD topologies are designed with coupled microstrip TLs [5, 10, 13, 14]. However, the resonant topologies do not permit to fully understand the NGD effect in electronics engineering. Other categories of non-resonant NGD circuits were also studied accordingly [17–22]. The basic property of NGD topologies was theoretically and experimentally demonstrated in the time-domain by operating with time-advanced baseband signals without causality principle's violation [16–20].

For a broad understanding, a fundamental NGD circuit theory inspired from the filter one was initiated [21]. It should be stressed that the main differences between the NGD circuits and filters are as follows: the filter specification is based on the magnitude and the NGD is characterized from the GD response. One can distinguish two classes of NGD topologies. The first class are the low-pass (LP) type NGD functions [16–25], usually dedicated to Hz or kHz frequency bands operations, which are susceptible to operating in baseband frequencies from DC. In the second class we find NGD circuits usually found in RF and microwave engineering operate with modulated signals where transmitted envelopes are measured in time-advance [5–14]. Nevertheless, the NGD effect is not known and/or understood by most electronic engineers. For this reason, further research works enabling the NGD circuit theory for non-specialist electronic design and manufacturing engineers are needed [22–27].

* Corresponding author: Blaise Ravelo (blaise.ravelo@yahoo.fr).

This paper identifies an operation enabling methodology for elementary first-order L-topology in the NGD or positive GD (PGD) modes. The reconfigurable positive/negative delay (RPND) cell of first-order passive topology constituted by RC-network, which, to the best of our knowledge, was never identified before, is the main object of this paper. The paper's organization is as follows:

- Section 2 describes the analyses of the identified simplest RPND topology of RC-network.
- Section 3 focuses on the design, prototyping and the time-domain test technique.
- Section 4 discusses on the validation study of the RPND circuit theory with time-advance experimentation.
- Section 5 is dedicated to the state-of-the-art comparative study with the existing NGD circuits.
- And the final conclusion is made in Section 6.

2. CIRCUIT ANALYSIS OF RC-NETWORK BASED RPND TOPOLOGY

The analytical study of the circuit topology that presents simplest RPND behavior is examined in this section.

2.1. LP-NGD Analysis of Identified PNRD Elementary Cell

The simplest elementary cell can be designed based on the use of a first-order admittance, represented by a conductance $(1/R)$ in parallel with a susceptance (B) defined by:

$$Y(s) = \frac{1}{R} + Bs \tag{1}$$

Therefore, the elementary cell topology under consideration is formed by parallel R_1C_1- and R_2C_2-networks. The schematic of this RPND cell is presented in Fig. 1.

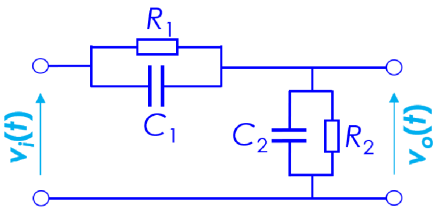

FIGURE 1. RPND $R_1C_1R_2C_2$-cell.

The Transfer Function (TF) of this circuit can be expressed in the following first-order form:

$$H(s) = T_0\frac{1+st_n}{1+st_d} \tag{2}$$

where T_0 is the DC attenuation, and t_n and t_d are the time constants associated with the numerator and denominator, respectively. These parameters are determined by the circuit component values with their specific expressions given as follows:

- The DC attenuation:

$$T_0 = \frac{R_2}{R_1+R_2} \tag{3}$$

- The TF numerator time constant:

$$t_n = R_1C_1 \tag{4}$$

- And the TF denominator time constant:

$$t_d = \frac{R_1R_2(C_1+C_2)}{R_1+R_2} \tag{5}$$

These delay time constants play on the reflected the combined energy storage and phase delay effect caused by the two RC branches. In the subsequent GD analysis, a key derived parameter:

$$t_0 = t_d - t_n \tag{6}$$

can be obtained from the basic parameters above. Substituting (4) and (5) into (6), we have:

$$t_0 = \frac{R_1(R_2C_2 - R_1C_1)}{R_1+R_2} \tag{7}$$

This parameter t_0 directly determines the circuit's group delay characteristics. A detailed mathematical analysis of the TF's frequency response will be examined in the next subsection.

2.2. Delay and NGD Cut-off Frequency Expressions Versus RC-parameters

We emphasize from previous formula (7) that the RPND cell behaves as LP-NGD function if:

$$R_2C_2 \leq R_1C_1 \tag{8}$$

otherwise the circuit exhibit a PGD. Then, the NGD cut-off frequency is formulated as:

$$f_0 = \frac{1}{2\pi R_1}\sqrt{\frac{R_1+R_2}{C_1R_2(C_1+C_2)}} \tag{9}$$

The design equations of RPND cell RC-network parameters are established in the next section as a function of algebraic delay ζ which can be negative $(\zeta \leq 0)$ or positive $(\zeta > 0)$ and attenuation $A < 1$. Under the particular case $C_1 = C_2 = C$, the GD and cut-off frequency are restated to:

$$t_0 = \frac{R_1C(R_2-R_1)}{R_1+R_2} \tag{10}$$

$$f_0 = \frac{1}{2\pi R_1C}\sqrt{\frac{R_1+R_2}{2R_2}} \tag{11}$$

We remark that the term t_0 is obviously negative when $R_1 > R_2$. Fig. 2(a) and Fig. 2(b) show the semi-log scale plots illustrating variation $t_0/(R_1C)$ and f_0R_1C versus R_1/R_2 ratio, where R_1/R_2 varies from 0.01 to 100.

We can emphasize that the quantities $t_0/(R_1C)$ and f_0R_1C decrease monotonically in the range of considered ratio R_1/R_2.

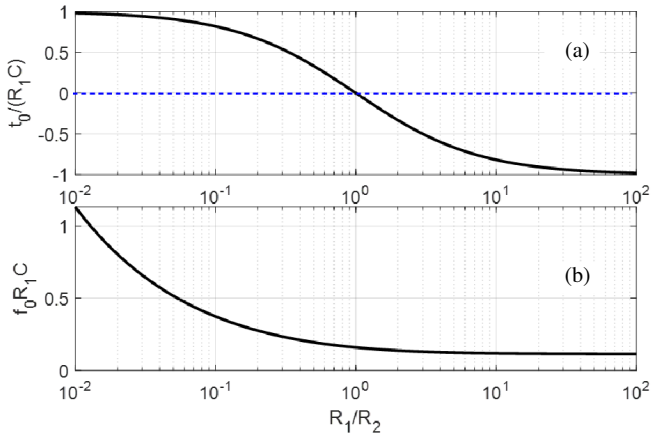

FIGURE 2. Plots of (a) $t_0/(R_1C)$ and (b) $f_0/(R_1C)$ versus R_1/R_2.

2.3. Design Equations of RPND RC-network Cell

To design the proposed RPND cell, we fix the capacitors C_1 and C_2 as given parameters. The resistor synthesis formulas are established by extracting R_1 and R_2 from Equations (12) and (13) with $T_0 = A$ and $t_0 = \zeta$:

$$R_1 = R_2\left(\frac{1}{A} - 1\right) \tag{12}$$

$$R_2 = \frac{A\zeta}{(1-A)[A(C_1+C_2)-C_1]} \tag{13}$$

For this circuit to be feasible, then $R_2 > 0$, which leads us to the following synthesis relations between A, C_1 and C_2 with respect to the GD:

- In the NGD ($\zeta \leq 0$) mode, we have:

$$A(C_1+C_2)-C_1 < 0 \;\Rightarrow\; A < A_{\max} = \frac{C_1}{C_1+C_2} \tag{14}$$

- In the PGD ($\zeta > 0$) mode, we have:

$$A(C_1+C_2)-C_1 > 0 \;\Rightarrow\; A > A_{\min} = \frac{C_1}{C_1+C_2} \tag{15}$$

Figure 3 displays the logarithmic scale mapping of optimal attenuation A_{opt} versus capacitors considered using $C_{\min}$ and $C_{\max}$ as boundary conditions.

We can find that A_{opt} varies between -40.09 dB to -0.09 dB when capacitors C_1 and C_2 are between 10 nF to 1 µF.

In the next section, we verify experimentally the developed RPND circuit theory.

3. DESIGN, PROTOTYPING AND EXPERIMENTAL SETUP OF THE RPND CIRCUIT THEORY

The design and implementation of RPND LP-NGD circuit prototype is described in this section. The simulated and measured PNRD prototype test results are discussed.

3.1. Numerical Analysis of the LP-NGD Circuit Synthesis

The RPND circuit prototype was designed to generate a NGD $\zeta = -3$ ms by using surface mounted capacitors $C_1 = 4.7$ µF and $C_2 = 2.2$ µF. According to (14), we should have $A_{\max} = -3.35$ dB and by means of Equation (12), we have:

$$R_{1\,\min} = \frac{A_{\max}}{1-A_{\max}}R_2 \tag{16}$$

Using the aforementioned condition, we find $R_{1\,\min} \approx 2.136R_2$. Tunable potentiometers with $R_{\max} = 10\,\text{k}\Omega$ were used to implement. The mapping of t_0 (resp. f_0) versus pair (R_1, R_2) is displayed in Fig. 4(a) (resp. Fig. 4(b)).

We can clearly see in this cartography the RPND evidence indicated by the area with positive and negative value of t_0. To behave as LP-NGD (resp. PGD) function, $R_{1\text{NGD}} = 1012\,\Omega$ (resp. $R_{1\text{PGD}} = 100\,\Omega$) and $R_{2\text{NGD}} = 323\,\Omega$ were considered during the test.

3.2. Description of the LP-NGD Circuit Prototype

The schematic designed in LTspice® simulator environment is depicted in Fig. 5(a). The printed circuit board (PCB) has physical size 43.4 mm × 11.2 mm with SMA connectors. The PCB photograph representing the RPND RC-network prototype is shown in Fig. 5(b).

The experimental test technique of the RPND circuit prototype is discussed in the next subsection.

3.3. LP-NGD Test Technique

The time-domain experimental tests were performed with arbitrary waveform input signals uploaded to control the signal generator (SG) Agilent 33220A. Thus, the input test signal was provided by the arbitrary wave SG. The input and output results are recorded by the oscilloscope as illustrated by Fig. 6. The employed digital oscilloscope is referenced Agilent DSO9404A with 4 GHz bandwidth and 20 Gsa/s.

The test results are discussed in the following section.

4. DISCUSSION ON THE VALIDATION RESULTS

The present section discusses both the frequency-domain and time-domain validation of the RCPND circuit theory.

4.1. RPND Frequency Domain Validation Results

During the experimentation, the input sine signal frequency was tuned up to 140 Hz. The calculated (or simulated with LTspice(r)) and measured frequency domain results in comparison are plotted in black solid curve and in req square dot curve, respectively. The calculated and measured magnitudes and GDs are excellently well-correlated. The obtained magnitude and GD responses of NGD and PGD mode are displayed in Figs. 7(a), 7(b), 7(c) and 7(d), respectively. The theoretical and measured results are in good agreement and confirm the validity of RNRD LP-NGD in the frequency domain.

The slight differences are mainly due to the measurement inaccuracies and systematic errors. Table 1 summarizes the comparison of calculated and tested NGD (resp. PGD) parameters

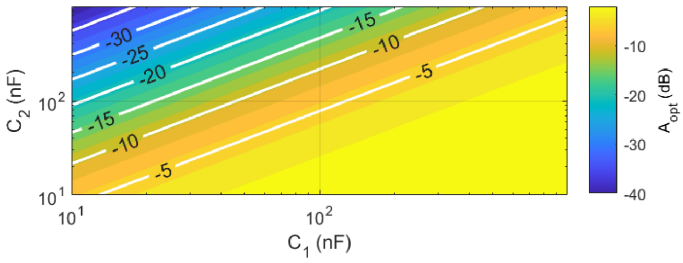

FIGURE 3. Mapping of A_{opt} versus pair (C_1, C_2).

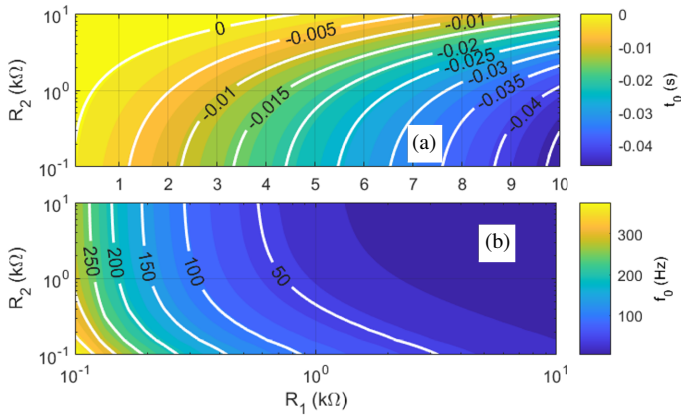

FIGURE 4. Cartographies of (a) t_0 and (b) f_0 versus (R_1, R_2) with fixed capacitors $C_1 = 4.7\,\mu\text{F}$ and $C_2 = 2.2\,\mu\text{F}$.

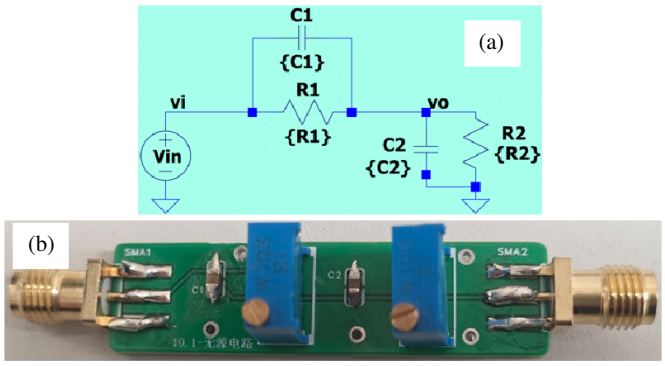

FIGURE 5. (a) Schematic and (b) photo of reconfigurable RPND circuit prototype.

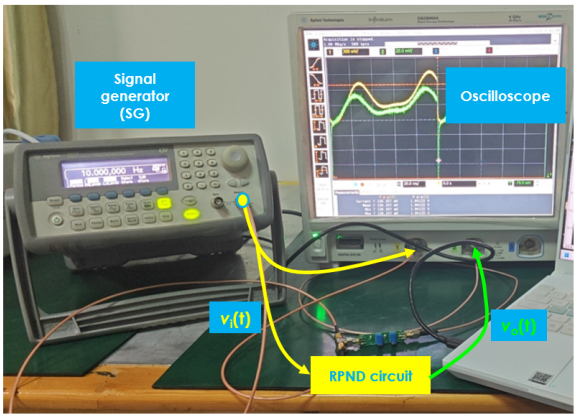

FIGURE 6. Experimental setup of reconfigurable PNRD circuit prototype.

T_{0n}, t_{0n} and f_{0n} (resp. T_{0p}, and t_{0p}). Despite the experimental result imperfection, a good agreement between measurement and simulation is observed.

More relevant verification of LP-NGD aspect based on time-domain analysis is studied in the next subsection.

4.2. Time-domain Validation Results

The validation results are based on the experimentation with arbitrary waveform signals. The following subsections are focused on the discussion about the obtained time-domain results.

4.2.1. Description of RPND Characterization Input Test Signals

The time-domain validation was carried out by injecting two different 1-V voltage signals into the RPND LP-NGD circuit prototype according to the experimental setup illustrated by Fig. 6. It is important to notice that the LP-NGD characterization is performed by the comparison of normalized input and output signals as follows:

$$\begin{cases} v_{i,normalized}(t) = \frac{v_i(t)}{\max[v_i(t)]} \\ v_{o,normalized}(t) = \frac{v_o(t)}{\max[v_o(t)]} \end{cases} \tag{17}$$

The RPND validation test results are discussed in the next paragraphs.

4.2.2. RPND Prototype Test Results with Pulse Input Signal

The obtained transient simulation results from LTspice® and measurement are displayed in Fig. 8.

The simulated and measured outputs plotted in red solid curve and blue-sky dashed curve, respectively, appears in time-advance of respective input in black solid, and navy-blue dashed curves. Fig. 8(a) represents the comparison truncated 1-V amplitude cosine pulse signal with 60 ms time duration. The rise (resp. fall) front time-advance is obviously seen in zoom in plot depicted by Fig. 8(b) (resp. Fig. 8(c)).

The LP-NGD calibration from the results shown in Fig. 8(a) enables to assess the simulated and tested time-advance t_{0time} determined graphically from the instant time of voltage equal to half-maximum given by equations:

$$\begin{cases} v_{i,normalized}(t = t_{in}) \approx 1/2 \\ v_{o,normalized}(t = t_{out}) \approx 1/2 \\ t_{0time} = t_{out} - t_{in} \end{cases} \tag{18}$$

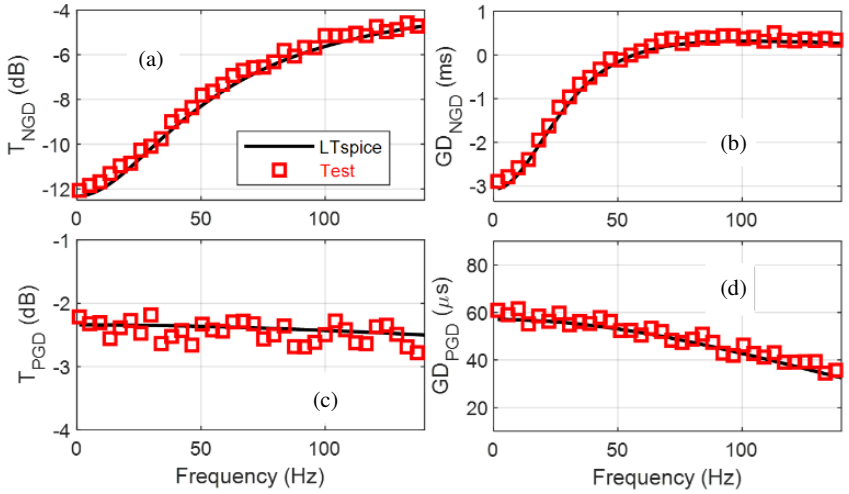

FIGURE 7. Measured amplitude and GD responses in NGD and PGD modes. (a) Amplitude response in NGD mode. (b) GD response in NGD mode. (c) Amplitude response in PGD mode. (d) GD response in PGD mode.

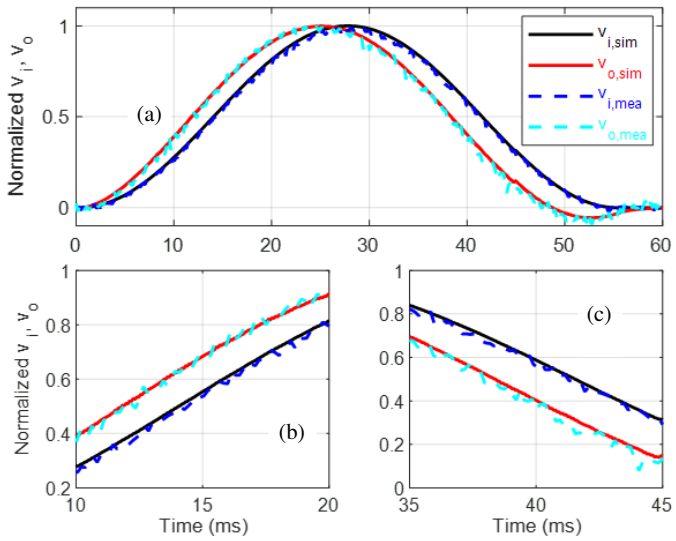

FIGURE 8. Time-advance experimental results of pulse in time intervals (a) [0, 60] ms, (b) [10, 20] ms and (c) [35, 45] ms.

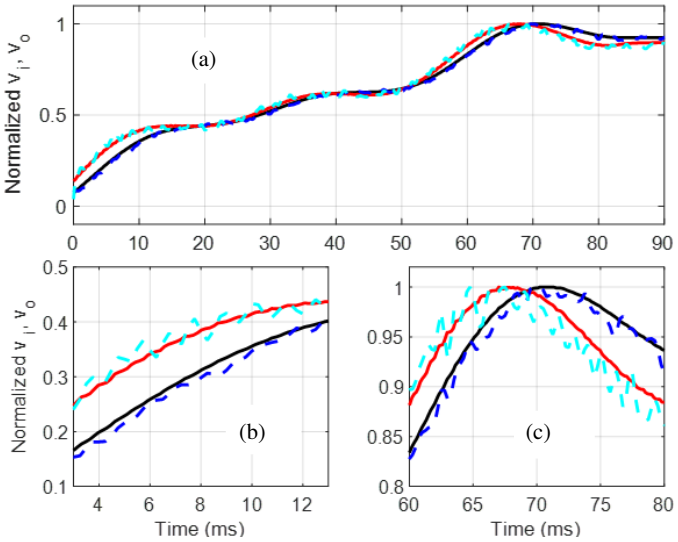

FIGURE 9. Time-advance experimental results of arbitrary waveform in the time intervals (a) [0, 90 ms], (b) [3.5, 12.5] ms and (c) [60, 80] ms.

and correlation coefficient which is determined from the "corrcoef" Matlab® instruction compared in Table 2.

In addition to the pulse signal test, time-domain investigation with more general signal waveform is discussed in the next paragraph.

4.2.3. Test Results with Arbitrary Waveform Input Signal

Figure 9(a) plots the comparison of transient simulation responses compared to the measured ones with completely arbitrary waveform input within a 90 ms time interval.

A good correlation between simulation and test results is obtained and confirm the LP-NGD function of prototype shown in Fig. 5. Moreover, the time-advance validation is clearly observed in zoom in showing rise front plot of Fig. 9(b) in [3.5, 12.5] ms and concave signal part zoomed in [60, 80] ms displayed in Fig. 9(c).

5. PNRD MODE CIRCUIT COMPARISON WITH EXISTING NGD CIRCUITS

The present comparative study is based on NGD lumped circuits constituted by RC- and RL-networks. NGD active circuits using operational amplifiers (OAs) [16–18, 20] and low-noise amplifier (LNA) [19] are also considered. As illustrated by Table 3, the studies on NGD circuits [20–22] available in the literature are only focused on the NGD mode aspect.

However, non-specialist engineers are wondering about the possibility to experiment circuits able to operate from PGD (normal) into NGD mode. Therefore, it is particularly important to show the feasibility study of RPND reconfigurability with a simple topology.

As application of the present research, the RPND RC topology has a particularly good potential of integration in electronic and communication systems in order to control the delay effect which helps in the control of destructive and constructive con-

TABLE 1. Comparison of frequency domain specifications of the RPND prototype.

Approach	t_{0n} (ms)	T_{0n} (dB)	f_{0n} (Hz)	t_{0p} (µs)	T_{0p} (dB)
LTspice®	−3.1	−12.31	56.1	57	−2.34
Test	−2.9	−12.02	55	60.2	−2.8

Specification	Time-advance (ms)	Correlation coefficient
Simulation	−2.8 ms	99.5%
Test	−2.7 ms	92.3%

TABLE 2. LP-NGD specifications from time-domain simulation and test of pulse signal shown in Fig. 8(a).

Reference	Topology	NGD	PGD
[17]	RC with OA	Yes	No
[16, 18]	RLC with OA	Yes	No
[19]	RC with LNA	Yes	No
[20]	RC with OA	Yes	No
[21]	RC with transistor	Yes	No
[22]	RL	Yes	No
This work	RC	Yes	Yes

TABLE 3. PNRD mode-based comparison of NGD circuit topologies available in the literature.

tributions of even and odd mode signals, another useful application is the integration in array antennas to create beam steering effect based solely on the transmission line compensated GD.

6. CONCLUSION

An original circuit theory of RPND topology is developed. The RPND topology is able to operate in the NGD- and PGD-modes.

The developed framework was focused on identifying the simplest elementary passive circuit represented by L-topology and first-order TF. The GD based frequency domain analysis allows to demonstrate that the identified RPND L-cell is constituted by series R_1C_1- and shunt R_2C_2-parellel networks. The existence condition of LP-NGD behavior in function of RPND topology RC parameters was established, with further evaluation of the design equations allowing to determine the RPND cell RC-parameters.

The RPND circuit theory was validated by the design and fabrication of a PCB prototype and experimental test in both frequency and time domain. The simulated and measurement results are in good agreement, confirming the RPND theory validity. Moreover, pulse and arbitrary experimental tests highlighted the possibility to generate time-advance aspects when the RPND circuit is reconfigured as LP-NGD function.

The RPND circuit is useful in the future for the signal synchronization by the design of a reconfigurable delay communication system.

ACKNOWLEDGEMENT

This research work is supported by NSFC research program in part by Grant No. 62350610268 and in part Grant No. 62371241.

REFERENCES

[1] Chu, S. and S. Wong, "Linear pulse propagation in an absorbing medium," *Physical Review Letters*, Vol. 48, No. 11, 738, 1982.

[2] Segard, B. and B. Macke, "Observation of negative velocity pulse propagation," *Physics Letters A*, Vol. 109, No. 5, 213–216, 1985.

[3] Macke, B. and B. Ségard, "Propagation of light-pulses at a negative group-velocity," *The European Physical Journal D — Atomic, Molecular, Optical and Plasma Physics*, Vol. 23, No. 1, 125–141, Apr. 2003.

[4] Macke, B., B. Ségard, and F. Wielonsky, "Optimal superluminal systems," *Physical Review E*, Vol. 72, No. 3, 035601(R), 2005.

[5] Monti, G. and L. Tarricone, "Negative group velocity in a split ring resonator-coupled microstrip line," *Progress In Electromagnetics Research*, Vol. 94, 33–47, 2009.

[6] Bukhman, N. S. and S. V. Bukhman, "On the negative delay time of a narrow-band signal as it passes through the resonant filter of absorption," *Radiophysics and Quantum Electronics*, Vol. 47, No. 1, 68–76, 2004.

[7] Bai, Y., Z. Wang, Y. M. Meng, H. Liu, and S. Fang, "A compact dual-band negative group delay circuit with independently adjustable characteristics," in *2021 Photonics & Electromagnetics Research Symposium (PIERS)*, 1807–1811, Hangzhou, China, Nov. 2021.

[8] Chaudhary, G., P. Kim, J. Kim, Y. Jeong, and J. Lim, "Coupled line negative group delay circuits with very low signal attenuation and multiple-poles characteristics," in *2014 44th European Microwave Conference*, 25–28, Rome, Italy, Oct. 2014.

[9] Kandic, M. and G. E. Bridges, "Asymptotic limits of negative group delay in active resonator-based distributed circuits," *IEEE Transactions on Circuits and Systems I: Regular Papers*, Vol. 58, No. 8, 1727–1735, Aug. 2011.

[10] Das, R., Q. Zhang, and H. Liu, "Lossy coupling matrix synthesis approach for the realization of negative group delay response," *IEEE Access*, Vol. 6, 1916–1926, Dec. 2017.

[11] Sánchez-Soriano, M. A., J. Durá, S. Sirci, and S. Marini, "Signal-interference-based structure with negative group delay properties," in *2018 48th European Microwave Conference (EuMC)*, 1021–1024, Madrid, Spain, Sep. 2018.

[12] Kayano, Y. and H. Inoue, "Embedded F-SIR type transmission line with open-stub for negative group delay characteristic," *IEICE Transactions on Electronics*, Vol. E99-C, No. 9, 1023–1026, Sep. 2016.

[13] Ravelo, B., F. Wan, N. Li, Z. Xu, P. Thakur, and A. Thakur, "Diakoptics modelling applied to flying bird-shape NGD microstrip

circuit," *IEEE Transactions on Circuits and Systems II: Express Briefs*, Vol. 68, No. 2, 637–641, Feb. 2021.

[14] Wan, F., N. Li, B. Ravelo, N. M. Murad, and W. Rahajandraibe, "NGD analysis of turtle-shape microstrip circuit," *IEEE Transactions on Circuits and Systems II: Express Briefs*, Vol. 67, No. 11, 2477–2481, Nov. 2020.

[15] Groenewold, G., "Noise and group delay in active filters," *IEEE Transactions on Circuits and Systems I: Regular Papers*, Vol. 54, No. 7, 1471–1480, Jul. 2007.

[16] Mitchell, M. W. and R. Y. Chiao, "Negative group delay and "fronts" in a causal system: An experiment with very low frequency bandpass amplifiers," *Physics Letters A*, Vol. 230, No. 3-4, 133–138, Jun. 1997.

[17] Nakanishi, T., K. Sugiyama, and M. Kitano, "Demonstration of negative group delays in a simple electronic circuit," *American Journal of Physics*, Vol. 70, No. 11, 1117–1121, 2002.

[18] Abuelma'atti, M. T. and Z. J. Khalifa, "A new CFOA-based negative group delay cascadable circuit," *Analog Integrated Circuits and Signal Processing*, Vol. 95, No. 2, 351–355, 2018.

[19] Wan, F., N. Li, B. Ravelo, J. Ge, and B. Li, "Time-domain experimentation of NGD ActiveRC-network cell," *IEEE Transactions on Circuits and Systems II: Express Briefs*, Vol. 66, No. 4, 562–566, Apr. 2019.

[20] Ravelo, B., H. Bilal, S. Rakotonandrasana, M. Guerin, F. Haddad, S. Ngoho, and W. Rahajandraibe, "Transient characterization of new low-pass negative group delay RC-network," *IEEE Transactions on Circuits and Systems II: Express Briefs*, Vol. 71, No. 1, 126–130, Jan. 2024.

[21] Ravelo, B., "Similitude between the NGD function and filter gain behaviours," *International Journal of Circuit Theory and Applications*, Vol. 42, No. 10, 1016–1032, Oct. 2014.

[22] Ravelo, B., W. Rahajandraibe, M. Guerin, B. Agnus, P. Thakur, and A. Thakur, "130-nm BiCMOS design of low-pass negative group delay integrated RL-circuit," *International Journal of Circuit Theory and Applications*, Vol. 50, No. 6, 1876–1889, Jun. 2022.

[23] Wan, F., T. Gu, B. Li, B. Li, W. Rahajandraibe, M. Guerin, S. Lalléchère, and B. Ravelo, "Design and experimentation of inductorless low-pass NGD integrated circuit in 180-nm CMOS technology," *IEEE Transactions on Computer-Aided Design of Integrated Circuits and Systems*, Vol. 41, No. 11, 4965–4974, Nov. 2022.

[24] Ravelo, B., J. Nebhen, M. Guerin, G. Chan, and W. Rahajandraibe, "Tensorial-analysis-of-networks applied to bandpass negative-group-delay analysis of resistorless LC-coupler-network," *Radio Science*, Vol. 57, No. 4, 1–13, Apr. 2022.

[25] Ravelo, B., H. Bilal, S. Rakotonandrasana, M. Guerin, F. Haddad, S. Ngoho, and W. Rahajandraibe, "Transient characterization of new low-pass negative group delay RC-network," *IEEE Transactions on Circuits and Systems II: Express Briefs*, Vol. 71, No. 1, 126–130, Jan. 2024.

[26] Vauché, R., R. A. B. Mefteh, F. Haddad, J. Nebhen, W. Rahajandraibe, F. Wan, S. Lalléchère, and B. Ravelo, "Experimental time-domain study for bandpass negative group delay analysis with lill-shape microstrip circuit," *IEEE Access*, Vol. 9, 24 155–24 167, 2021.

[27] Vauché, R., R. A. B. Mefteh, F. Haddad, W. Rahajandraibe, F. Wan, S. Lalléchère, G. Fontgalland, P. Thakur, A. Thakur, and B. Ravelo, "Bandpass NGD time-domain experimental test of double-Li microstrip circuit," *IEEE Design & Test*, Vol. 39, No. 2, 121–128, 2022.